Electronic Supplementary Material (ESI) for Journal of Materials Chemistry A.
This journal is © The Royal Society of Chemistry 2022

Electronic Supplementary Material (ESI) for Journal of Materials Chemistry A.
This journal is © The Royal Society of Chemistry

Supplementary Information

Covalent organic framework based multifunctional self-sanitizing face masks

Luo-Gang Ding,[‡a] Song Wang,[‡b] Bing-Jian Yao,[*a] Wen-Xiu Wu,[a] Jing-Lan Kan,[a] Yueyue Liu,[b] Jiaqiang Wu,[*b] and Yu-Bin Dong[*a]

List of Content

1. Synthesis and characterization of 5,10,15,20-tetra-(4-aminophenyl)porphyrin (Tph)

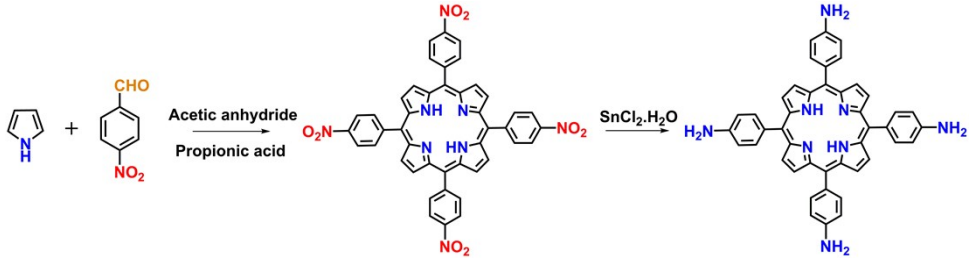

Tph was synthesized according to the modified literature method.[1] Briefly, 4-nitrobenzaldehyde (11.0 g, 72.5 mmol) and acetic anhydride (12.0 mL, 127 mmol) was dissolved in propionic acid (300 mL). The solution was then refluxed, to which pyrrole (5.0 mL, 72 mmol) was slowly added. After refluxing for 30 min, the resulting mixture was cooled to give a precipitate which was collected by filtration, washed with H_2O and methanol, and dried under vacuum. The resulting powder was dissolved in pyridine (80 mL) which was refluxed for 1.0 h. After cooling, the precipitate was collected by filtration and washed with acetone to give 5,10,15,20-tetra-(4-nitrophenyl)porphyrin (Tph-NO_2) as a purple crystal in 15 wt % yield.

Tph-NO_2 (2 g, 2.52 mmol) was dissolved in hot HCl (245 mL) at 70 °C, to which was added $SnCl_2{\cdot}2H_2O$ (9.0 g, 40 mmol). The resulting mixture was stirred at 70 °C for 30 min and then cooled to 0 °C. After neutralization with ammonium hydroxide, the resulting gray crystalline was collected by filtration and dissolved in acetone. Rotary evaporation of the solution followed by drying under vacuum yielded Tph as a purple crystal in 85 wt % yield. IR (KBr): 3327 (s), 3214 (w), 3035 (m), 2923 (m),1611 (s), 1508 (s), 1465 (s), 1351 (m), 1279 (s), 1181 (s), 970 (s), 798 (s), 732 (s); ^{1}H-NMR spectrum (400 MHz, DMSO-d_6, ppm, δ): 8.88 (s, 8H, Ar H), 7.84~7.86 (d, 8H, CH), 6.99~7.01 (m, 8H, Ar H), 5.60 (s, 8H, NH_2), -2.75 (s, 2H, NH); ^{13}C-NMR spectrum (101 MHz, DMSO-d_6, ppm, δ) of Tph: 149.00, 135.94, 129.21, 121.05, 112.99; HRMS (ESI) *m/z*: $[M+H]^+$, Calcd for $C_{44}H_{34}N_8$, 675.2979; found, 675.2916.

2. Synthesis and characterization of isocyanate-terminated polyurethane oligomer (NCO-PU)

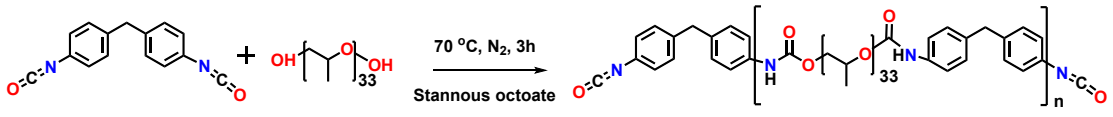

NCO-PU was synthesized according to our previous method.[2] Generally, polypropene oxide (PPO) was dried in vacuum at 80 °C for 24 h before use. PPO was placed in a glass-jacketed reactor (250 mL) and stirred at room temperature in a nitrogen atmosphere for 1.0 h, and then MDI was added with stirring (ratio of NCO:OH groups of 1.2:1). The mixture was heated at 70 °C for 3.0 h in nitrogen to afford the expected polyurethane oligomer, which was stored in a vacuum desiccator for later use. GPC with a Waters 515 system and 2410 refractive-index detector, calibrated with a narrow-molecular-weight polystyrene standard, was used to characterize the molecular weight of NCO-PU by using THF as the mobile phase. The number average molecular weight (*Mn*) and polydispersity (PDI) of NCO-PU was determined as 3235 Da and 1.50 respectively based on the GPC analysis. IR (KBr): 3405 (w), 3295 (w), 2975 (s), 2877 (s), 2280 (s),

1735 (m), 1605 (m), 1527 (s), 1459 (w), 1412 (m), 1373 (m), 1305 (w), 1236 (w), 1109 (s), 1020 (w), 926 (w), 822 (m).

3. Synthesis and characterization of model compound

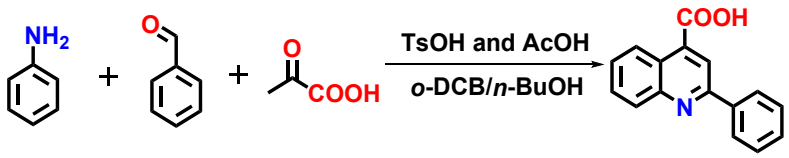

Scheme S1. Synthesis of model compound (*2-phenylquinoline-4-carboxylic acid*) via Doebner reaction.

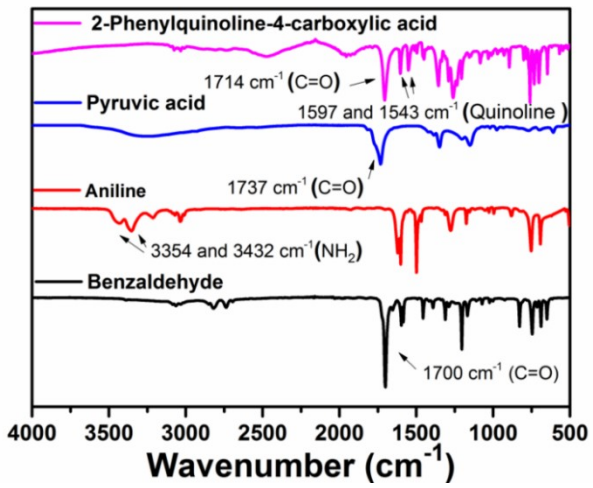

Fig. S1 FTIR (KBr, cm^{-1}) of *2-phenylquinoline-4-carboxylic acid*. The typical N-H vibration peaks at 3354 and 3432 cm^{-1} in aniline and the C=O vibration peak at 1700 cm^{-1} in benzaldehyde completely disappeared after reaction. Meanwhile, new characteristic peaks for C=N groups at 1597 and 1543 cm^{-1} demonstrated the formation of quinolyl moiety in the product. Additionally, the peak of 1714 cm^{-1} belonging to the carboxylic acid groups was also observed.

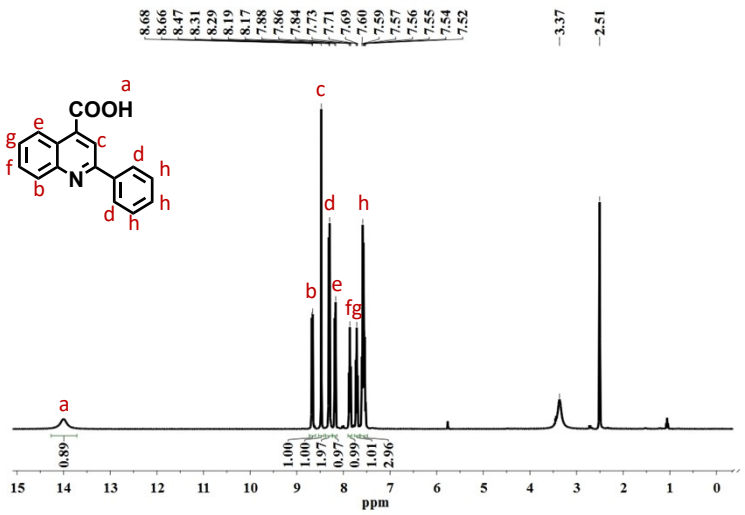

Fig. S2 ^{1}H-NMR spectrum (400 MHz, DMSO-d_6, ppm) of *2-phenylquinoline-4-carboxylic acid*: δ 14.00 (s, 1H, COOH), 8.68, 8.66 (d, 1H, Ar H), 8.47 (s, 1H, CH), 8.31, 8.29 (d, 2H, Ar H), 8.19-8.17 (d, 1H, Ar H), 7.88-7.84 (t, 1H, Ar H), 7.71-7.69 (t, 1H, Ar H), 7.60-7.52 (m, 3H, Ar H).

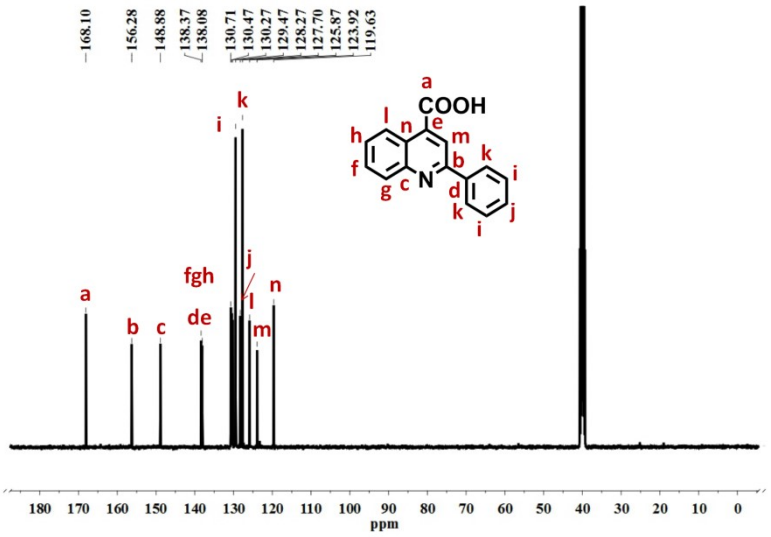

Fig. S3 ^{13}C-NMR spectrum (101 MHz, DMSO-d_6, ppm) of *2-phenylquinoline-4-carboxylic acid*: δ 168.10, 156.28, 148.88, 138.37, 138.08, 130.71, 130.47, 130.27, 129.47, 128.27, 127.70, 125.87, 123.92, 119.63.

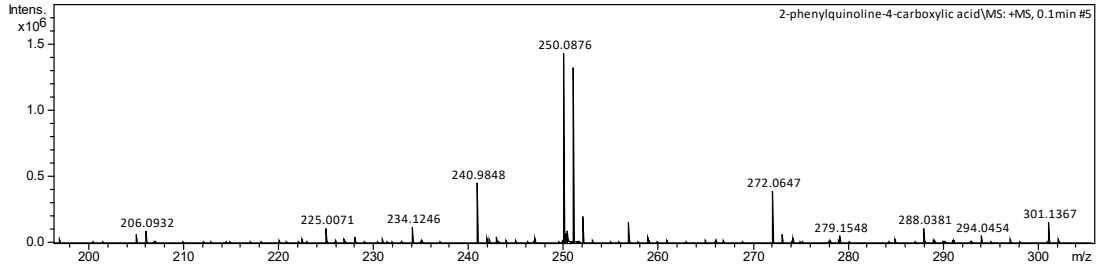

Fig. S4 HRMS spectrum (ESI) of *2-phenylquinoline-4-carboxylic acid*: *m/z*: $[M+H]^+$, Calcd for $C_{16}H_{11}NO_2$, 250.0790; found, 250.0876.

4. Synthesis and characterization of DhaTph-COOH and Ag@DhaTph-COOH

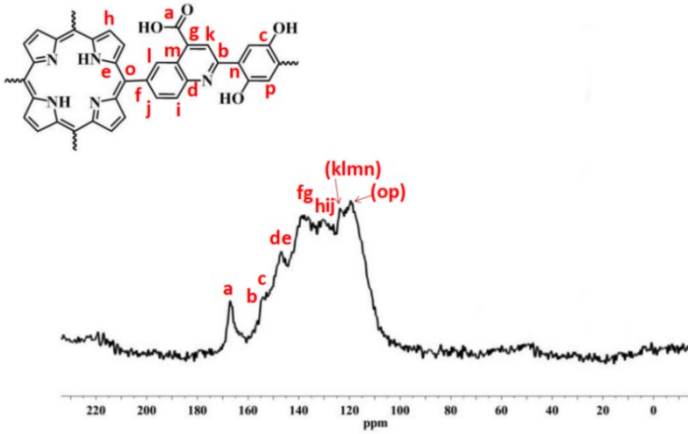

Fig. S5 ^{13}C CP-MAS NMR spectrum (400 MHz, ppm) of **DhaTph-COOH**: *δ* 167.5, 156.6, 151.7, 148.6, 147.1, 138.1, 136.5, 130.3, 128.1, 126.5, 123.8, 119.6.

Table S1 Fractional atomic coordinates for the unit cell of **DhaTph-COOH**.

AA stacking mode, space group: P_4							
$a = b$ = 36.1 Å, c = 4.2 Å, $\alpha = \beta = \gamma$ = 90.0 °, R_{wp} = 2.67 % and R_p = 1.71 %							
Atom	x	y	z	Atom	x	y	z
C1	0.97301	-1.60869	0.21714	C34	1.48942	-1.88422	-0.10449
C2	1.01098	-1.61158	0.21821	C35	1.47588	-1.91843	-0.01154
C3	0.9633	-1.57397	0.10454	N36	1.5043	-1.94186	0.04702
C4	1.06387	-1.57197	0.05127	C37	1.53581	-1.92254	-0.00552
C5	1.09047	-1.60391	0.05442	C38	1.43812	-1.9267	0.04332
C6	1.08314	-1.63579	-0.12441	C39	1.19923	-1.5957	0.54033
C7	1.10808	-1.66529	-0.12818	O40	1.22214	-1.59969	0.74935
C8	1.14154	-1.66272	0.03481	O41	1.18759	-1.55995	0.46664
C9	1.15029	-1.63051	0.21195	C42	1.3015	-1.90693	-0.41545
C10	1.12344	-1.60212	0.23095	O43	1.28332	-1.90305	-0.65511
N11	1.16582	-1.69132	0.01787	O44	1.30802	-1.94287	-0.31135
C12	1.19913	-1.69056	0.16541	O45	1.32009	-1.73764	-0.17981
C13	1.20938	-1.65935	0.33972	O46	1.17949	-1.7678	0.32106
C14	1.18544	-1.62869	0.36438	H47	0.95446	-1.63082	0.28334
C15	1.22484	-1.72194	0.1255	H48	1.02601	-1.6363	0.28366
C16	1.26075	-1.71514	0.00963	H49	1.05786	-1.6379	-0.25918
C17	1.28506	-1.74449	-0.05163	H50	1.10195	-1.69006	-0.26349
C18	1.2734	-1.78108	0.00149	H51	1.12758	-1.57829	0.37935
C19	1.23752	-1.78794	0.11633	H52	1.23636	-1.65863	0.45199
C20	1.21344	-1.75883	0.1827	H53	1.26958	-1.68709	-0.04075
C21	1.29952	-1.81198	-0.04188	H54	1.22835	-1.81591	0.16635
C22	1.28976	-1.84334	-0.2171	H55	1.26273	-1.84463	-0.32839
C23	1.31442	-1.8734	-0.24228	H56	1.37324	-1.92188	-0.27166
C24	1.34962	-1.87075	-0.09349	H57	1.44194	-1.86202	0.37674
C25	1.35762	-1.83874	0.08747	H58	1.39622	-1.81127	0.39428
N26	1.33272	-1.8108	0.10726	H59	1.46796	-1.99796	-0.12699
C27	1.37724	-1.89823	-0.11965	H60	1.5461	-1.86431	-0.14932
C28	1.41043	-1.89579	0.05243	H61	1.47387	-1.85947	-0.15959
C29	1.41679	-1.8644	0.24013	H62	1.20236	-1.54125	0.59438
C30	1.39092	-1.83575	0.25183	H63	1.32	-1.94347	-0.09223
C31	1.42139	-2.02579	0.10782	H64	1.32711	-1.71038	-0.18785
N32	1.44631	-1.99629	0.0348	H65	1.16557	-1.74586	0.41337
C33	1.52725	-1.88678	-0.09943				

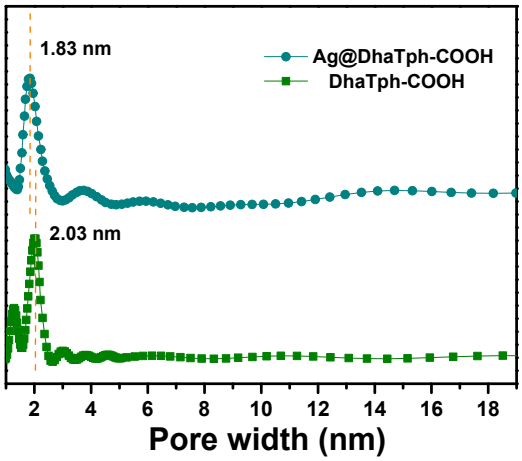

Fig. S6 Pore size distribution of **DhaTph-COOH** and **Ag@DhaTph-COOH** based on BET data.

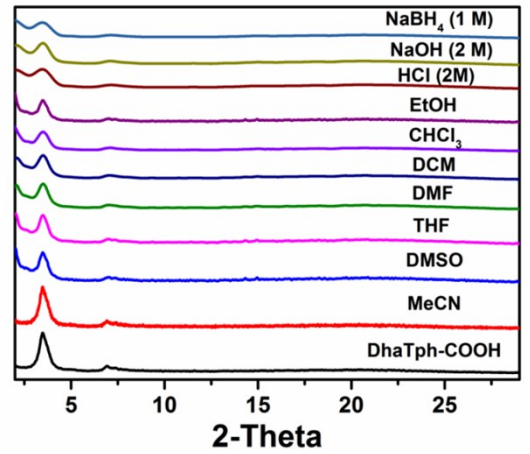

Fig. S7 Stability examination of **DhaTph-COOH** in different media (soaking in different media for 24 h).

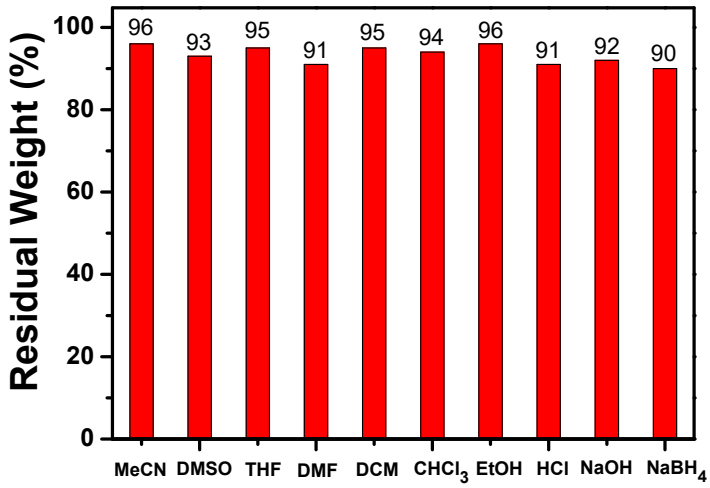

Fig. S8 Residual weight percentage of **DhaTph-COOH** after treatment in different solvents for 24 h.

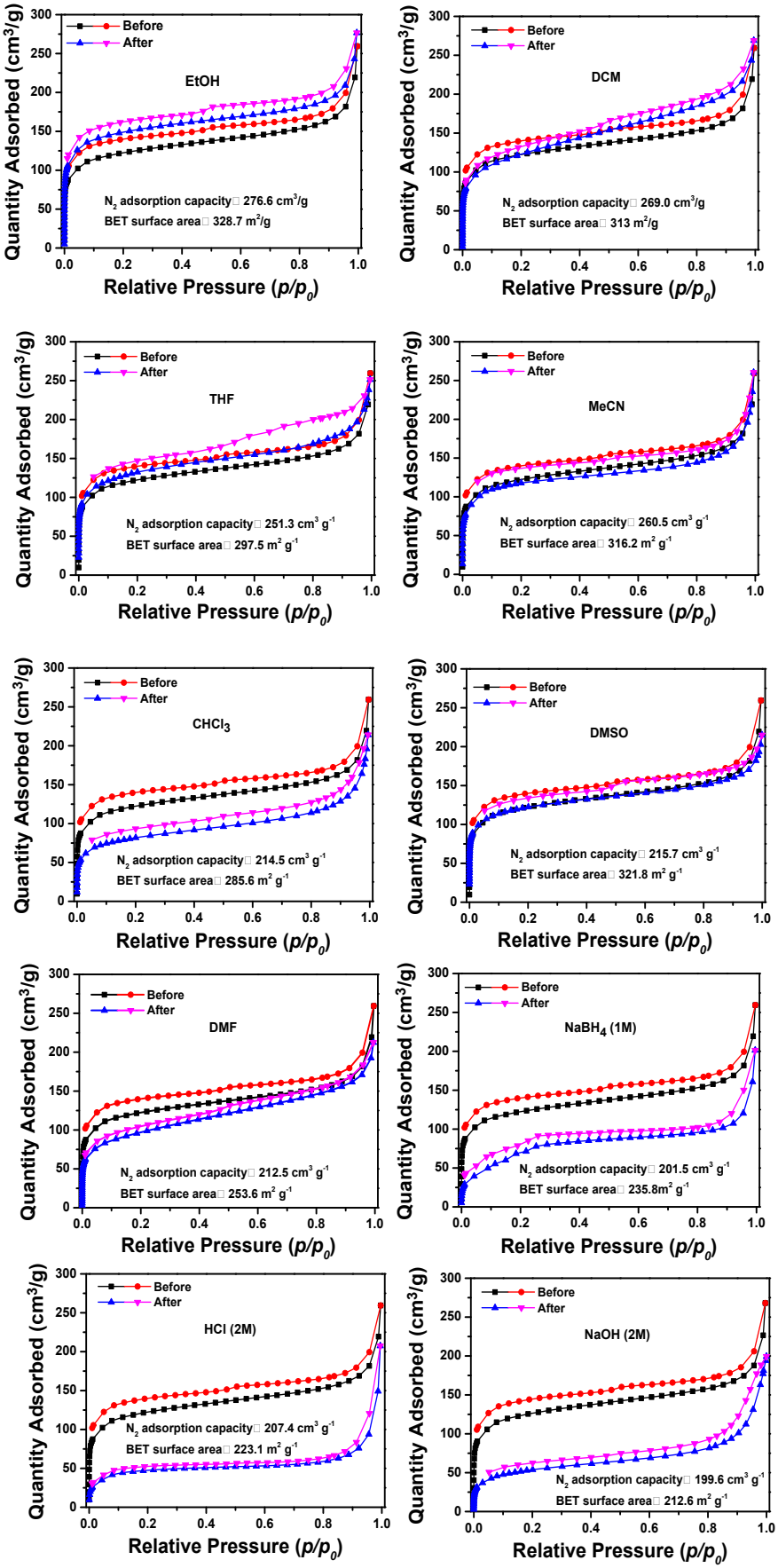

Fig. S9 N_2 adsorption and desorption isotherms of **DhaTph-COOH** after treatment with different solvents for 24 h.

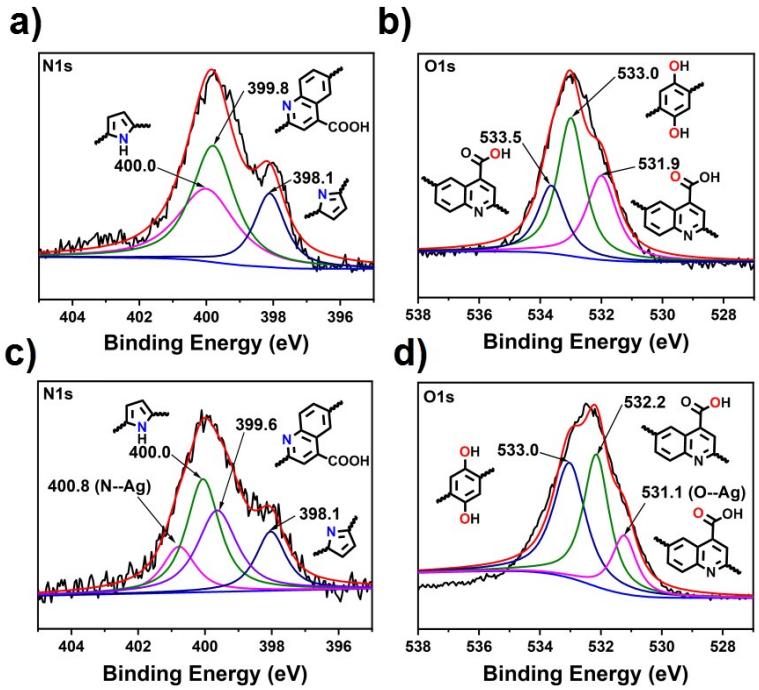

Fig. S10 a, c) N1s and b, d) O1s XPS spectra of **DhaTph-COOH** and **Ag@DhaTph-COOH**, respectively.

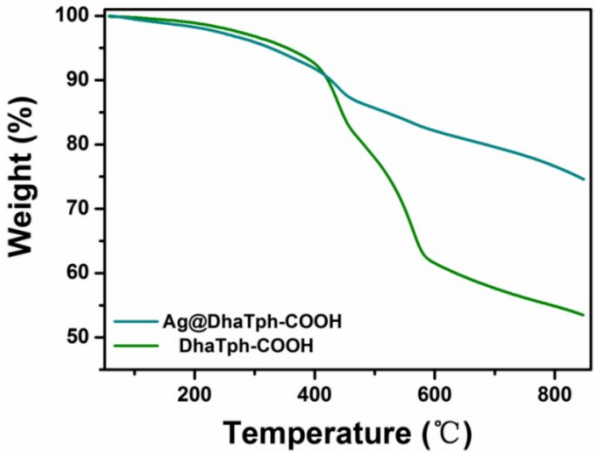

Fig. S11 TGA traces of **DhaTph-COOH** and **Ag@DhaTph-COOH**.

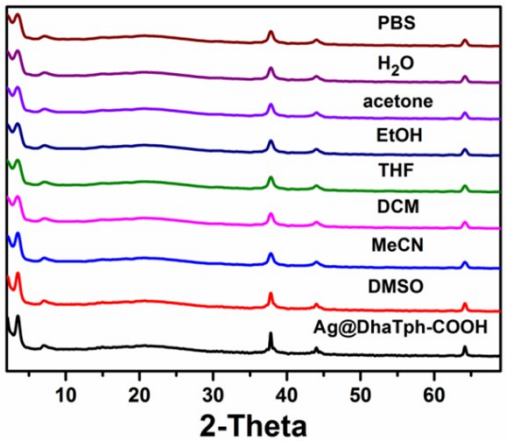

Fig. S12 Stability examination of **Ag@DhaTph-COOH** in different media (soaking in different media for 24 h).

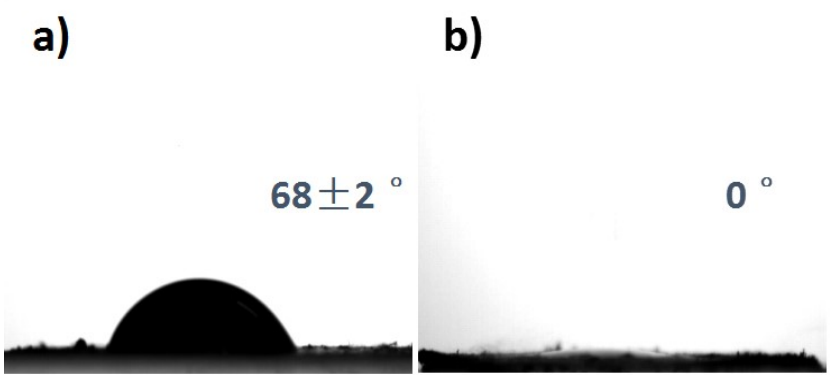

Fig. S13 Water contact angle (WCA) images of a) **DhaTph-COOH** and b) **Ag@DhaTph-COOH**.

5. PTT and PDT properties of DhaTph-COOH and Ag@DhaTph-COOH

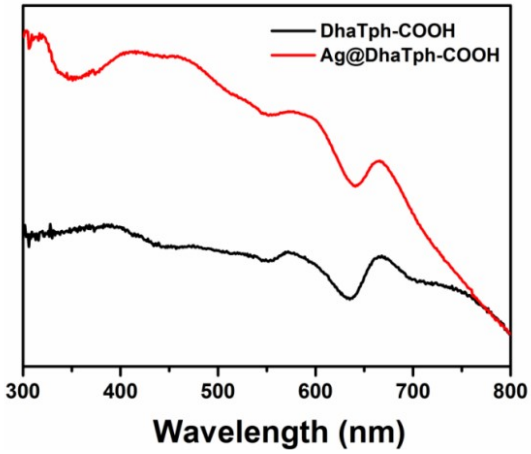

Fig. S14 Solid-state UV-Vis spectra of **DhaTph-COOH**, and **Ag@DhaTph-COOH**. Most of the absorption peaks are located above 400 nm, including porphyrin Soret band (ca. 426 nm) and weak Q-bands (518-702 nm).

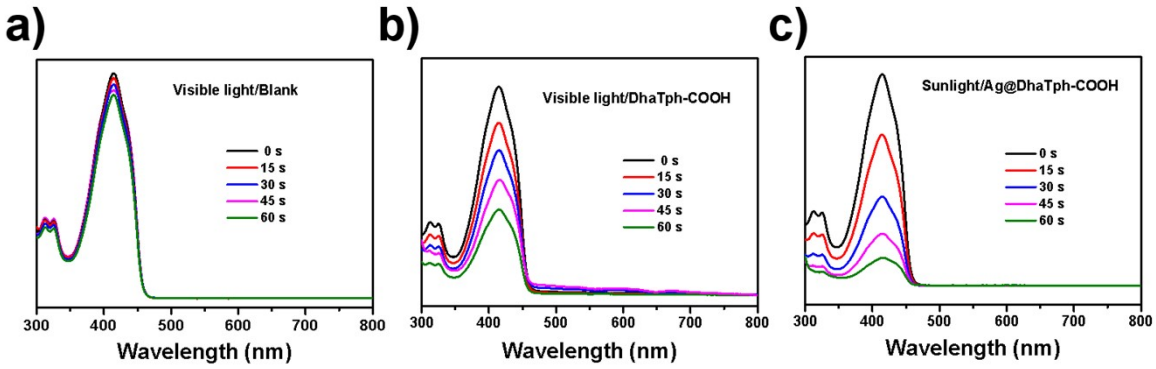

Fig. S15 Time-dependent $^1O_2$ generation kinetics of DPBF with different treatments (DPBF in DMF, 2.5 mM; **DhaTph-COOH**, 0.9 mg mL^{-1}; **Ag@DhaTph-COOH**, 1.0 mg mL^{-1}; visible light, $\lambda > 400$ nm, ca. 50 mW cm^{-2}; sunlight, 50-54 mW cm^{-2}).

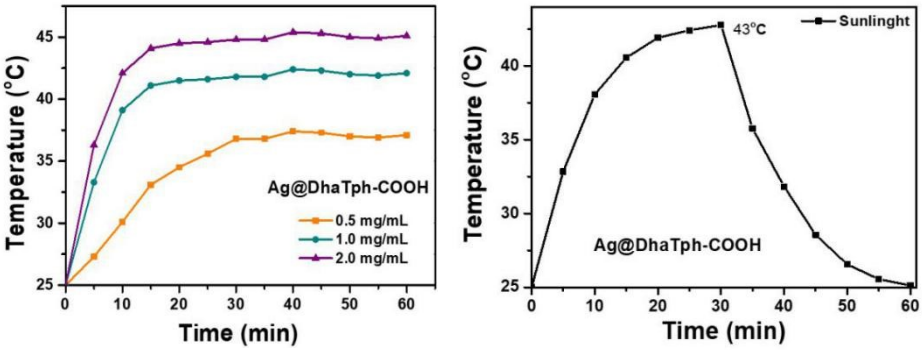

Fig. S16 Left: temperature increase induced by different concentrations of **Ag@DhaTph-COOH** under visible light irradiation in PBS. Right: temperature curve of **Ag@DhaTph-COOH** in PBS (1.0 mg mL^{-1}) measured by a thermocouple thermometer and recorded at 5 min intervals under sunlight irradiation (50-54 mW cm^{-2}).

6. Antibacterial and antiviral performance

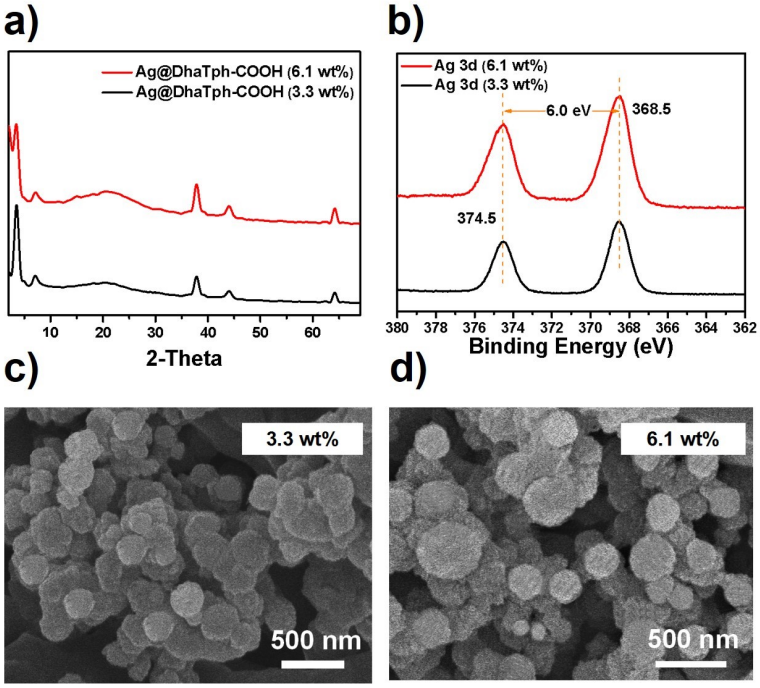

Fig. S17 a, b) The XRD and XPS spectrum of Ag 3d in **Ag@DhaTph-COOH** with 3.3 and 6.1 wt% of Ag species. c) SEM of **Ag@DhaTph-COOH** with 3.3 wt% of Ag species. d) SEM of **Ag@DhaTph-COOH** with 6.1 wt% of Ag species.

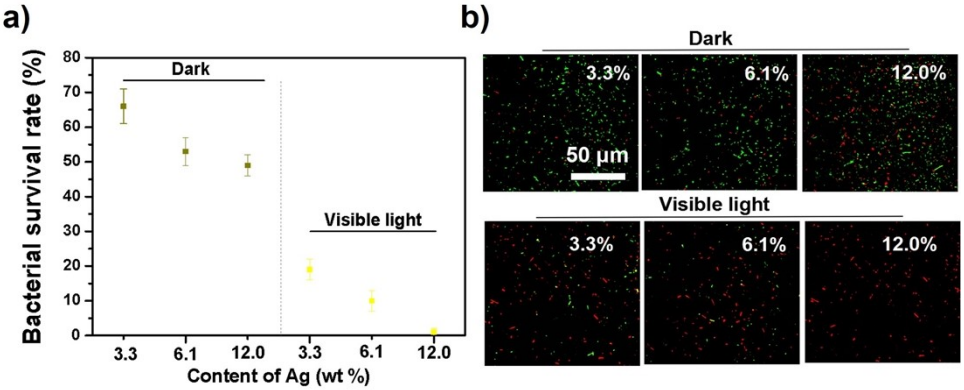

Fig. S18 a) Antibacterial effect of **Ag@DhaTph-COOH** with different Ag loading for 30 min under visible light (ca. 50 mW cm^{-2}, λ > 400 nm) irradiation and dark conditions. b) The live/dead bacterial fluorescent images of different groups against *E. coli.*

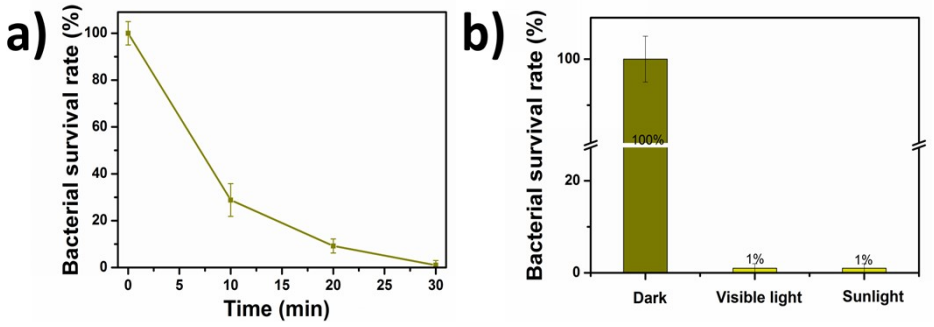

Fig. S19 a) Time examination of the antibacterial efficiency of **Ag@DhaTph-COOH** (1.0 mg) against *S. aureus* upon visible light irradiation (ca. 50 mW cm^{-2}, λ > 400 nm). b) The antibacterial efficiency of **Ag@DhaTph-COOH** (1.0 mg) under light treatment conditions within a fixed irradiation time of 30 min, compared without **Ag@DhaTph-COOH** in dark (visible light, λ > 400 nm, ca. 50 mW cm^{-2}; sunlight, 50-54 mW cm^{-2}).

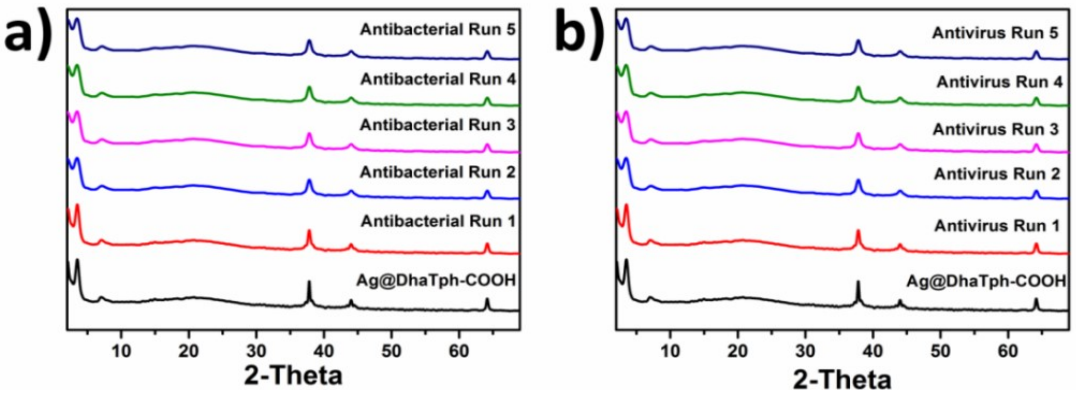

Fig. S20 PXRD patterns of **Ag@DhaTph-COOH** before and after a) antibacterial and b) antivirus runs.

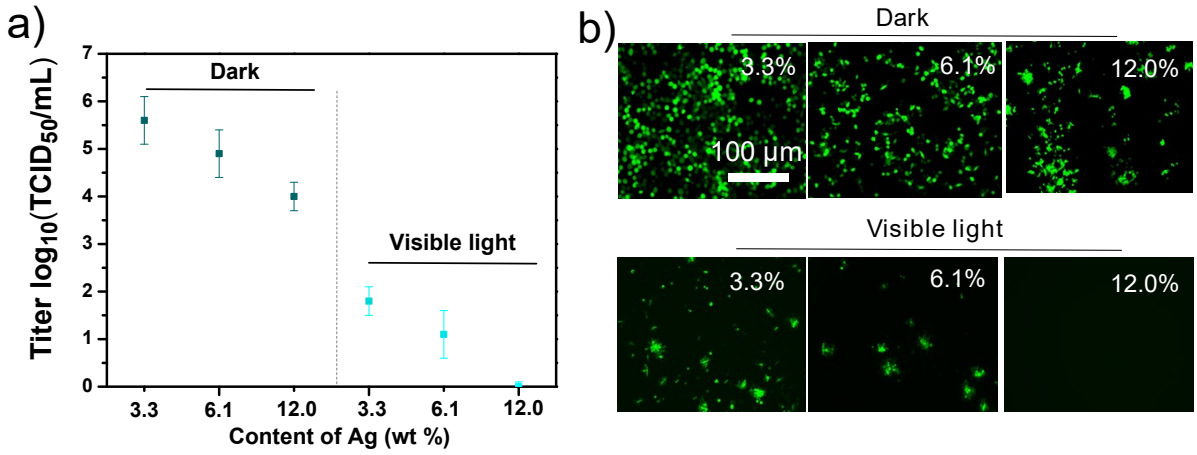

Fig. S21 a) Antiviral effect of **Ag@DhaTph-COOH** with different Ag loading for 60 min under visible light (ca. 50 mW cm^{-2}, λ > 400 nm) irradiation and dark conditions. b) Immunofluorescence assay of VSV-infected Hela cells treated by **Ag@DhaTph-COOH** with different Ag loading.

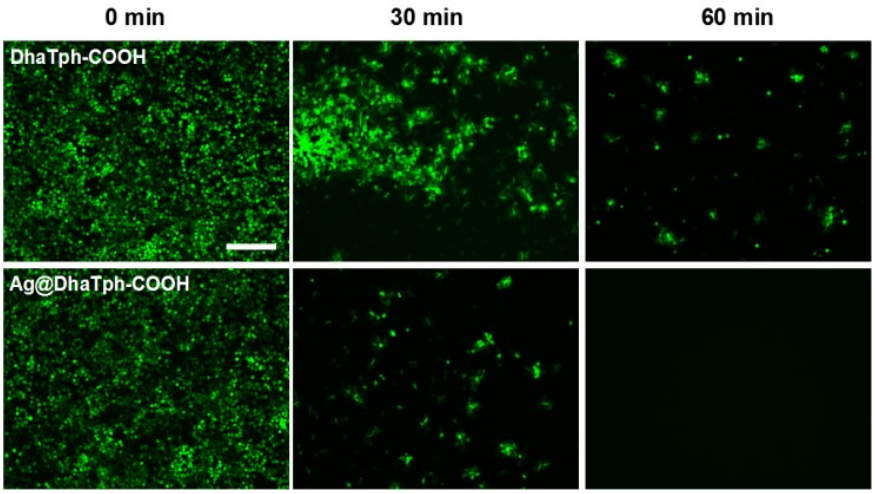

Fig. S22 Immunofluorescence assay of VSV-infected Hela cells treated with **DhaTph-COOH** (0.9 mg) and **Ag@DhaTph-COOH** (1.0 mg) respectively within different time periods upon visible light irradiation (ca. 50 mW cm^{-2}, λ > 400 nm), bar = 100 μm.

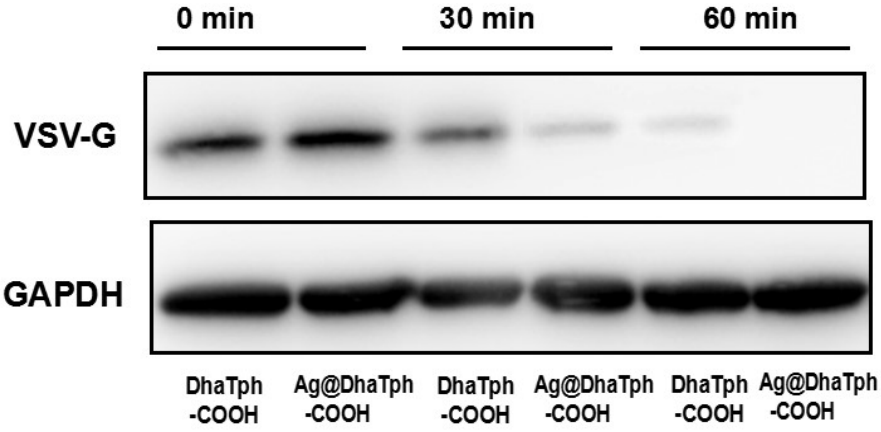

Fig. S23 VSV-G protein expression in the groups respectively treated with **DhaTph-COOH** (0.9 mg) and **Ag@DhaTph-COOH** (1.0 mg) upon visible light irradiation via Western blotting experiment (ca. 50 mW cm^{-2}, λ > 400 nm) within different time periods.

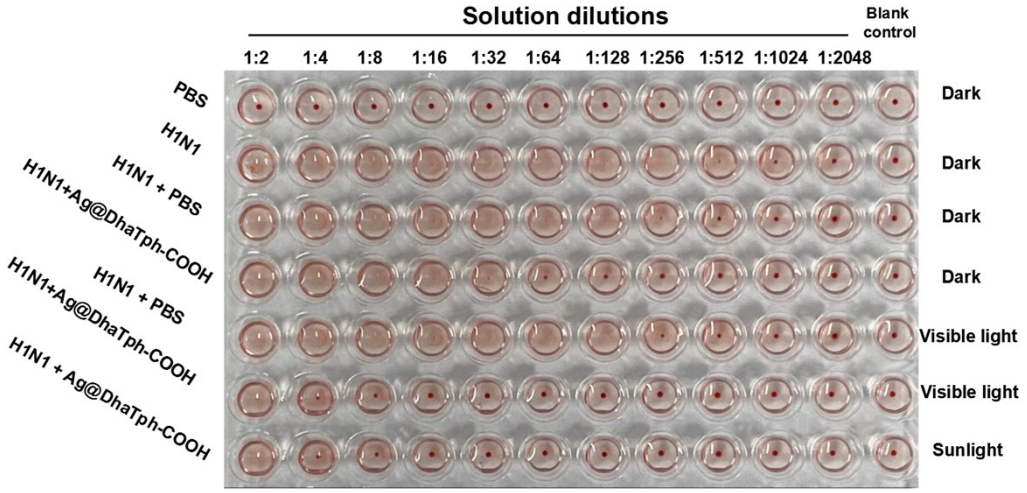

Fig. S24 Photographs of hemagglutination assay (HA) of different COF-treated groups against H1N1 under different conditions (*d* = 9.0 cm). General procedure:[3]

7. Fabrication and characterization of multifunctional self-sanitizing facemask

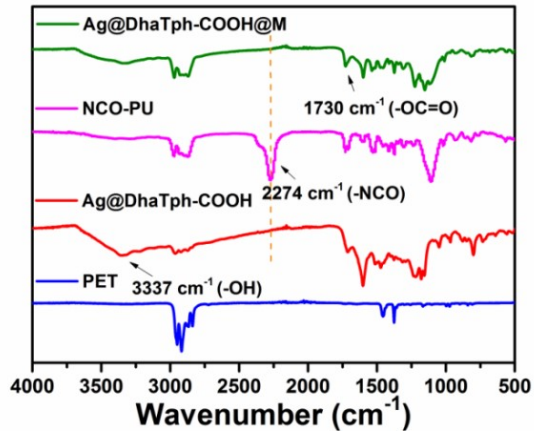

Fig. S25 FTIR spectra of **Ag@DhaTph-COOH@M** and the starting materials. The characteristic peak (2274 cm^{-1}) of the isocyanate group in NCO-PU disappeared completely after the reaction, and the relative intensity of the vibration absorption band (3337 cm^{-1}) belonging to hydroxyl group in **Ag@DhaTph-COOH** obviously decreased, indicating successful cross-linking between the NCO-terminated PU oligomers and OH-functionalized COF NPs.

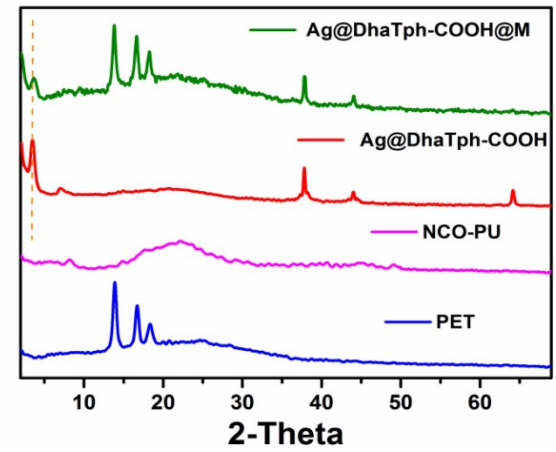

Fig. S26 PXRD patterns of **Ag@DhaTph-COOH@M** and the starting materials. The PXRD pattern of the **Ag@DhaTph-COOH@M** showed that the structural integrity and crystallinity of **Ag@DhaTph-COOH** were well maintained in the chemical crosslinking coating.

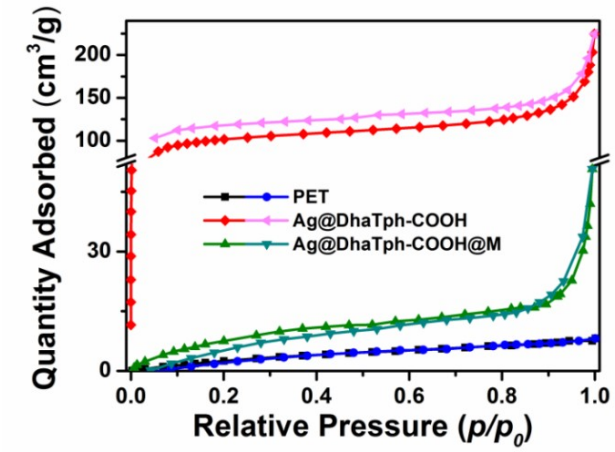

Fig. S27 N_2 adsorption isomers (at 77 K) of the PET, **Ag@DhaTph-COOH**, and **Ag@DhaTph-COOH@M**, respectively.

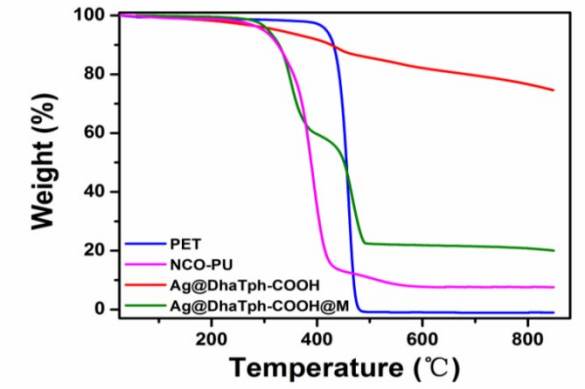

Fig. S28 TGA traces of **Ag@DhaTph-COOH@M** and the starting materials. As revealed by the TGA trace, **Ag@DhaTph-COOH@M** showed almost no weight loss up to 200 °C, indicating its good thermal stability.

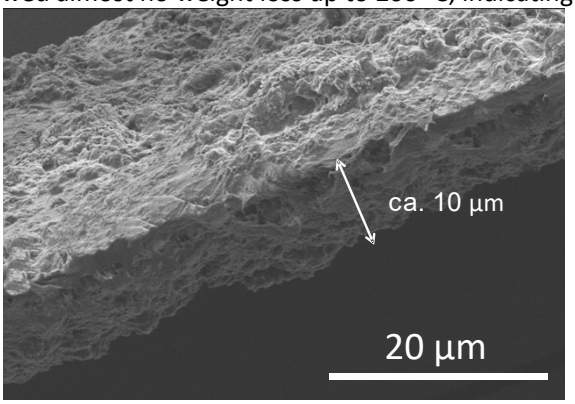

Fig. S29 Cross section of the stripped film from the COF-involved coating, the thickness measured is ca. 10 μm.

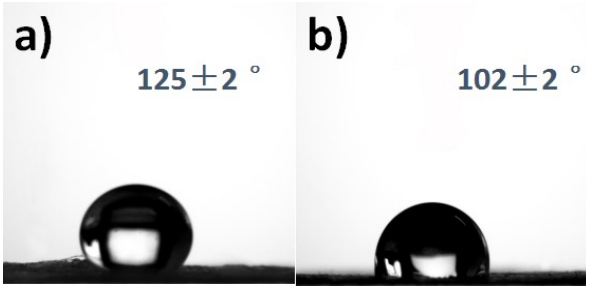

Fig. S30 Water contact angles (WCA) images of a) pristine mask cloth and b) **Ag@DhaTph-COOH@M**.

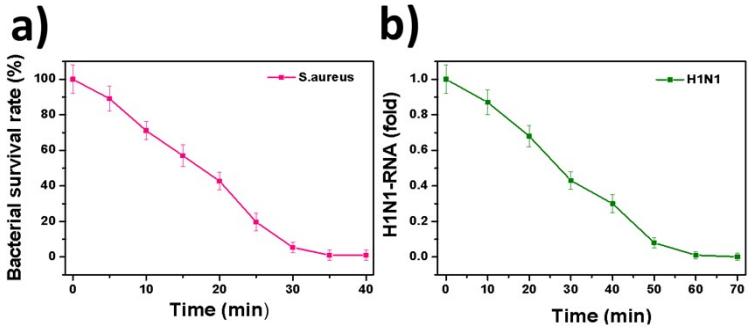

Fig. S31 Time examination of the survival rate of *S. aureus* and the level of H1N1-RNA over **Ag@DhaTph-COOH@M** under natural sunlight irradiation (50-54 mW cm^{-2}).

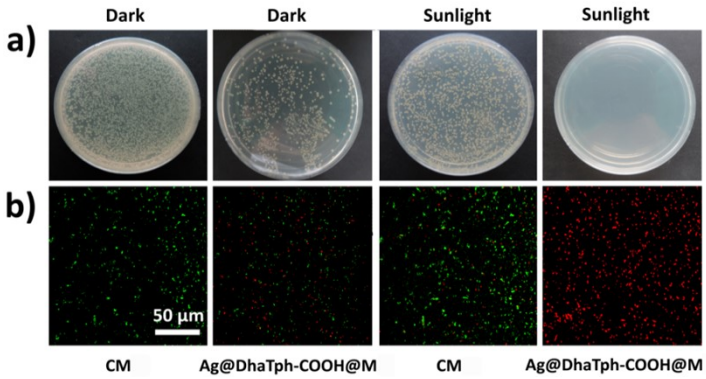

Fig. S32 Agar plate count and live/dead bacterial fluorescent images of *S. aureus* treated with **Ag@DhaTph-COOH@M** under natural sunlight irradiation in 35 min (50-54 mW cm^{-2}).

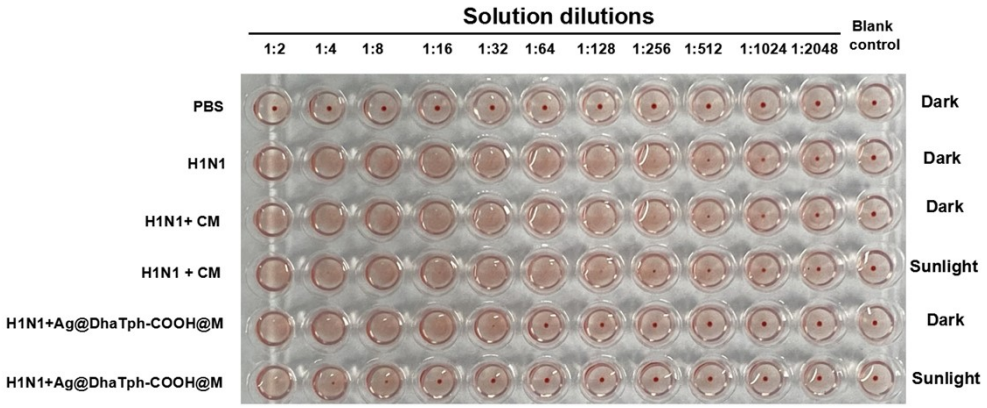

Fig. S33 The agglutinating activity of samples containing H1N1 treated with **Ag@DhaTph-COOH@M** and CM were subjected to a hemagglutination assay.

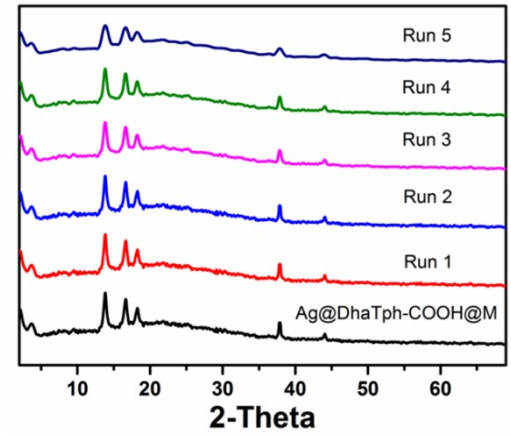

Fig. S34 PXRD patterns of **Ag@DhaTph-COOH@M** after each cycle.

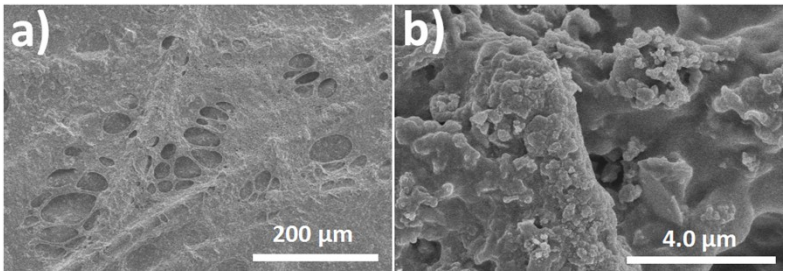

Fig. S35 SEM images of **Ag@DhaTph-COOH@M** after five cycles.

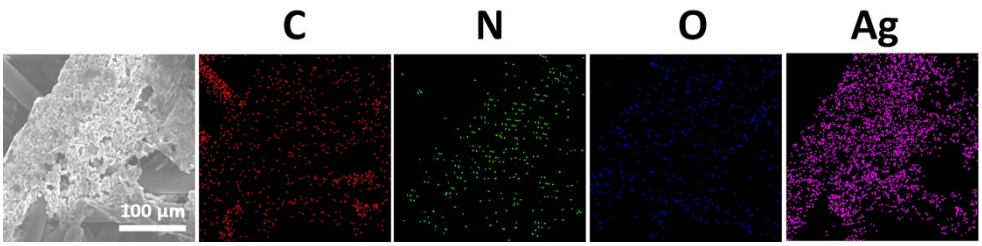

Fig. S36 SEM-EDX elemental mapping images of **Ag@DhaTph-COOH@M** after five cycles.

8. References

1 M. Yuasa, K. Oyaizu, A. Yamaguchi and M. Kuwakado, *J. Am. Chem. Soc*., 2004, **126**, 11128.

2 B. J. Yao, W. L. Jiang, Y. Dong, Z. X. Liu and Y. B. Dong, *Chem.-Eur. J.,* 2016, **22**, 10565.

3 A. J. Eisfeld, G. Neumann and Y. Kawaoka, *Nat. Protoc.,* 2014, **9**, 2663.